

## Hydrogen Bonding—New Insights

# CHALLENGES AND ADVANCES IN COMPUTATIONAL CHEMISTRY AND PHYSICS

---

Volume 3

---

Series Editor:

JERZY LESZCZYNSKI

*Department of Chemistry, Jackson State University, USA*

*The titles published in this series are listed at the end of this volume.*

# Hydrogen Bonding—New Insights

Edited by

SŁAWOMIR J. GRABOWSKI

*Department of Physics and Chemistry  
University of Łódź  
Poland*



Springer

A C.I.P. Catalogue record for this book is available from the Library of Congress.

ISBN-10 1-4020-4852-1 (HB)  
ISBN-13 978-1-4020-4852-4 (HB)  
ISBN-10 1-4020-4853-X (e-book)  
ISBN-13 978-1-4020-4853-1 (e-book)

Published by Springer,  
P.O. Box 17, 3300 AA Dordrecht, The Netherlands.

[www.springer.com](http://www.springer.com)

*Printed on acid-free paper*

All Rights Reserved

©2006 Springer

No part of this work may be reproduced, stored in a retrieval system, or transmitted in any form or by any means, electronic, mechanical, photocopying, microfilming, recording or otherwise, without written permission from the Publisher, with the exception of any material supplied specifically for the purpose of being entered and executed on a computer system, for exclusive use by the purchaser of the work.

## PREFACE

Hydrogen bond is a unique interaction whose importance is great in chemical and bio-chemical reactions including life processes. The number of studies on H-bonding is large and this is reflected by a vast number of different monographs and review articles that cover these phenomena. Hence the following question arises: what is the reason to edit the next book concerning hydrogen bond. The answer is simple, recent numerous studies and the quick and large development of both experimental as well as theoretical techniques cause that old monographs and review articles become quickly out of date.

It seems that presently the situation is similar to that one in the 1980s. Before that time the H-bond was understood in the sense of the Pauling definition as an electrostatic in nature interaction concerning three atoms—hydrogen atom located between two other electronegative ones and bounded stronger to one of them. Few studies were published where the authors found interactions which at least partly fulfill the classical definition of H-bond, as for example the Suttor studies in 1964 on  $C-H \cdots Y$  interactions in crystals. However, since C-atom in the proton-donating bond is not electronegative thus these systems are not in line with the classical definition. Also the other “typical” features of H-bonds for  $C-H \cdots Y$  systems are not always fulfilled. No surprisingly, only when the study of Taylor and Kennard (1982, *J. Am. Chem. Soc.* 104, 5063) based on the refined statistical techniques applied for the data taken from the Cambridge Structural Database appeared, the existence of  $C-H \cdots Y$  hydrogen bonds was commonly accepted. And since that time there was a forceful “jump” on the number of H-bond studies. Among others the  $C-H \cdots Y$ ,  $X-H \cdots C$  and  $C-H \cdots C$  interactions were investigated and their features were also compared with the so-called conventional hydrogen bonds. However, it is worth mentioning that very often the controversies and discussions are related to different meaning of H-bond and with the use of different definitions of that interaction. What are the unique features of H-bond interaction? We hope that the reader will find an answer within the chapters of this volume.

One can ask another important question: what is the current situation on investigations on H-bond? Recently, different kinds of interactions are analyzed which may be classified as hydrogen bonds; one can mention dihydrogen bonds or blue-shifting hydrogen bonds. There are new various theoretical methods. One of the most important tools often recently applied in studies on H-bonds is the “atoms in molecules” theory (AIM). It is worth mentioning the studies on the nature of H-bond interaction since the following questions arise

very often: are the H-bonds electrostatic in nature according to the Pauling definition? What are differences between different kinds of H-bonds since the H-bond energy ranges from a fraction to tens of kcal/mol? Is this energy difference the reason why very weak H-bonds are different in nature than the very strong ones? One can provide a lot of examples on new topics, new theoretical methods and new experimental techniques recently used in studies on H-bond interactions.

In this volume mainly the theoretical studies are presented, however also examples of experimental results are included and all the computational results are strongly related to experimental techniques. The most important topics considered in the recent studies on hydrogen bond are discussed in this volume, such problems as: how to estimate the energy of intramolecular H-bonds, covalency of these interactions, the distant consequences of H-bond since in earlier studies usually only the  $X-H \cdots Y$  H-bridge was analyzed ( $X-H$  is the proton-donating bond and  $Y$  is an acceptor), the differences between H-bond and van der Waals interactions from one side and covalent bonds from the other side, the use of the Bader theory to analyze different kinds of H-bonds, the influence of weak H-bonds upon structure and function of biological molecules, etc. There are also topics related to the experimental results: crystal structures, infrared and NMR techniques and many others.

It is obvious that in the case of such broad research area as hydrogen bond interactions it is very difficult to consider all aspects and discuss all problems. However, the authors of the chapters made an effort to consider all current topics and recent techniques applied in the studies of this important phenomenon. As an editor of this volume, I would like to thank the authors for their outstanding work. Their excellent contributions collected in this volume provide the readers the basis to systematize knowledge on H-bond interaction and new insights into hydrogen bonding.

Sławomir J. Grabowski  
Łódź, Poland  
December 2005

## COLOR PLATE SECTION

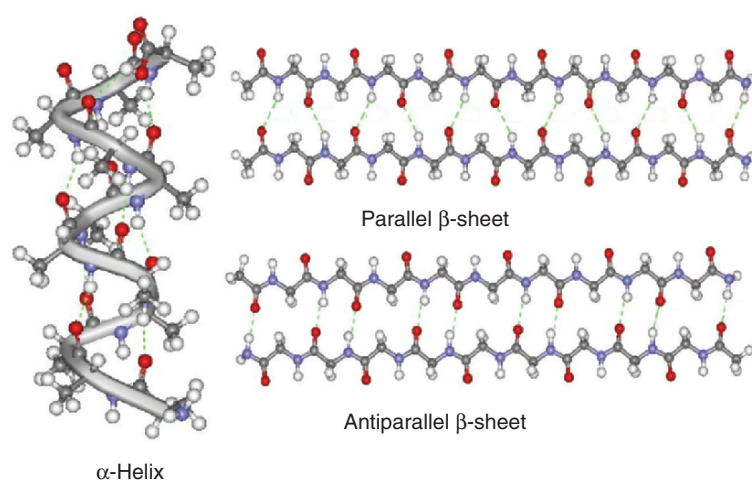


Figure 1-2. Hydrogen bonding in various protein secondary structures.

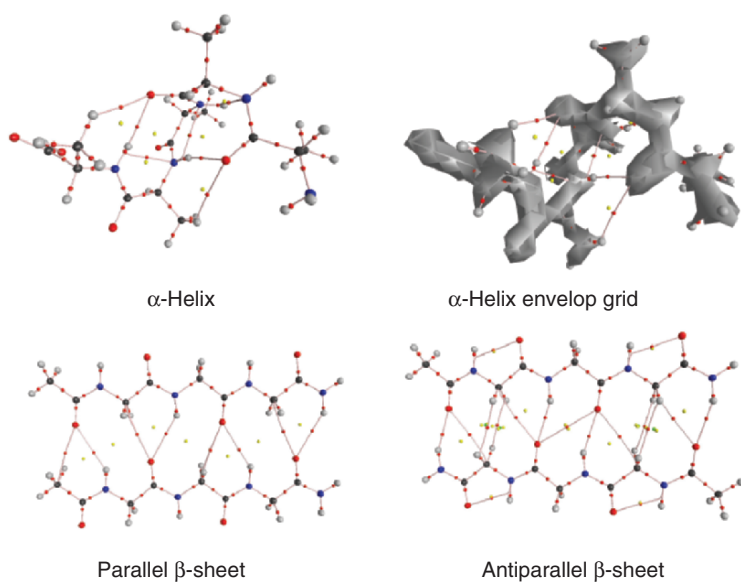


Figure 1-11. Molecular topographies of secondary structures of protein obtained from theoretical electron density. (Results from Ref. [325].)

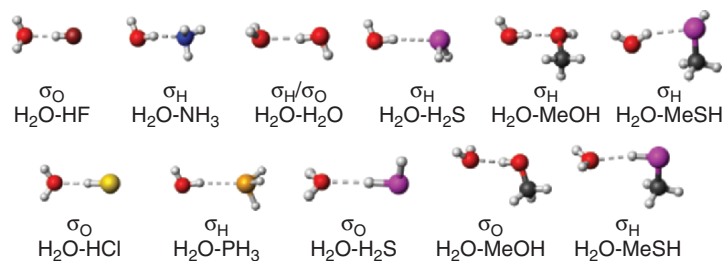


Figure 4-2. Structures of the hydrogen-bonded complexes of  $H_2O$ .

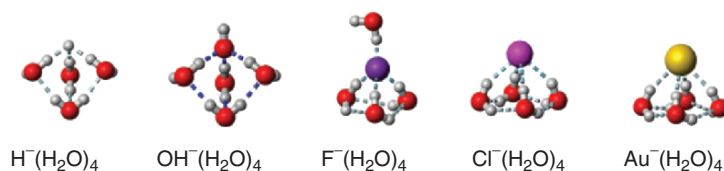


Figure 4-8. Structures of hydrated anion clusters.

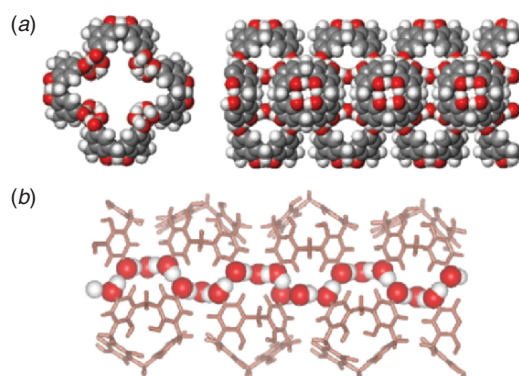


Figure 4-11. Longitudinal H-bond relay comprised of CHQs and water. (a) Tubular polymer structure of a single nanotube obtained with x-ray analysis for the heavy atoms and with ab initio calculations for the H-orientations (top and side views). (b) One of four pillar frames of short H-bonds represents a 1-D H-bond relay composed of a series of consecutive OH groups [hydroxyl groups ( $-OH$ ) in CHQs and the OHs in water molecules]. Reproduced by permission of American Chemical Society: Ref. [54].



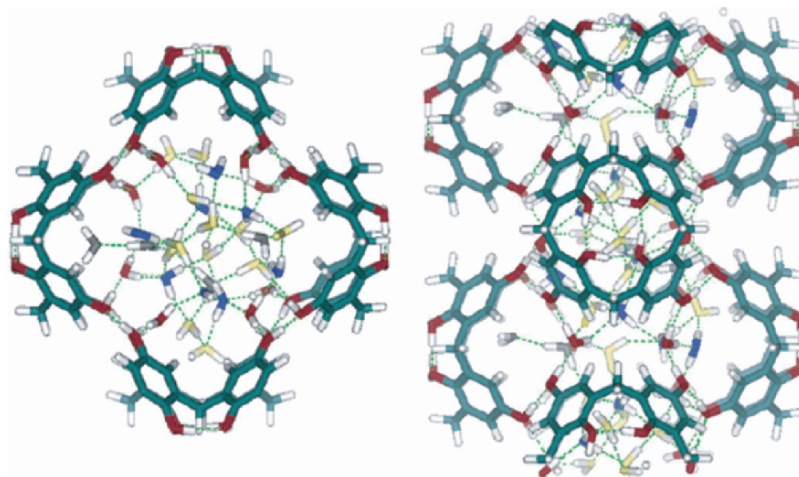


Figure 4-12. The water network in a single tube (top and side views). The top view (left) shows 8 bridging water molecules in red, 8 first-hydration shell water molecules in blue, 12 second-hydration shell water molecules in yellow, and 4 third-hydration shell water molecules in gray, while the side view shows twice those in the top view. Reproduced by permission of American Chemical Society: Ref. [54].

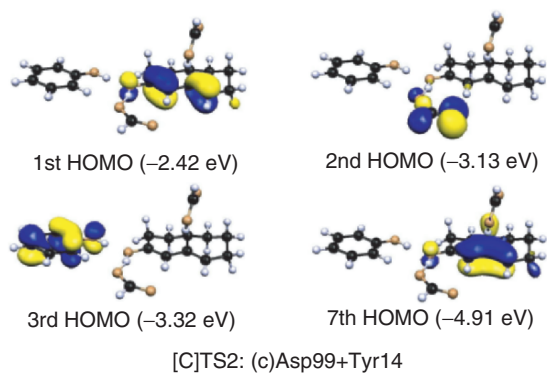


Figure 4-13. Schematic representation of reaction mechanism and HOMO energy levels of transition state (TS) of KSI.

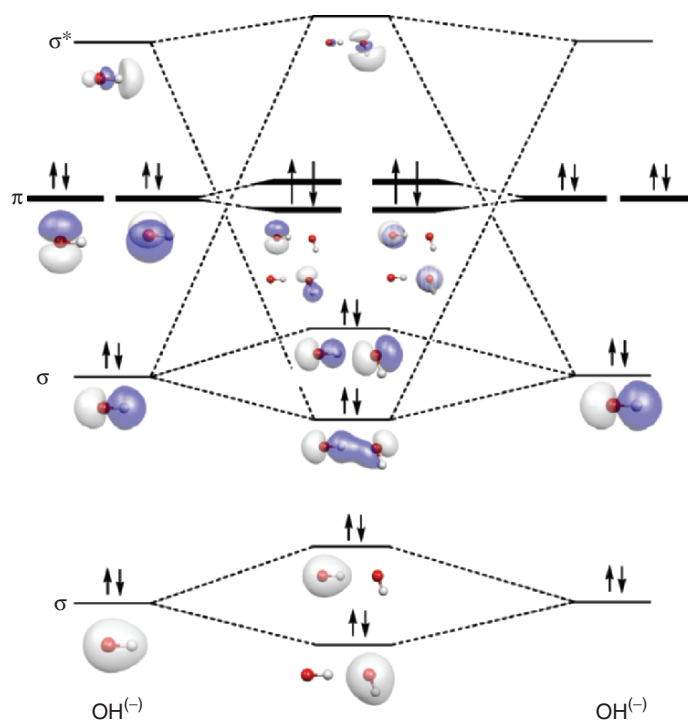


Figure 5-19. Orbital diagram of the interaction between two  $\text{OH}^{(-)}$  anions with their  $\text{O}-\text{H}\cdots\text{O}$  contact at the same geometry than the  $\text{O}-\text{H}\cdots\text{O}$  bond in the water dimer. See text for details.

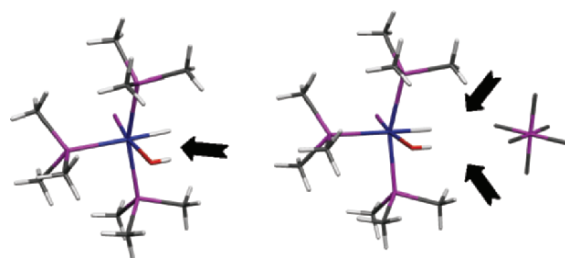


Figure 6-4. The x-ray structure of  $[\text{IrH}(\text{OH})(\text{PMe}_3)_4][\text{PF}_6]$ : cation (left) and cation and anion (right).

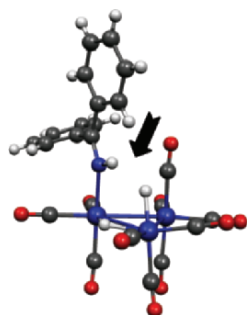


Figure 6-5. The x-ray structure of  $[\text{Os}_3(\text{CO})_{10}\text{H}(\mu\text{-H})(\text{HN}=\text{CPh}_2)]$ .

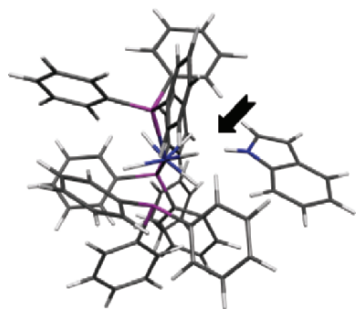


Figure 6-6. The neutron diffraction structure of  $[\text{ReH}_5(\text{PPh}_3)_3]\cdot\text{indole}\cdot\text{benzene}$ .

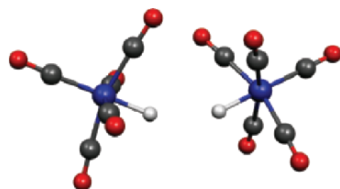


Figure 6-7. The neutron diffraction structure of  $[\text{MnH}(\text{CO})_5]$  dimer.

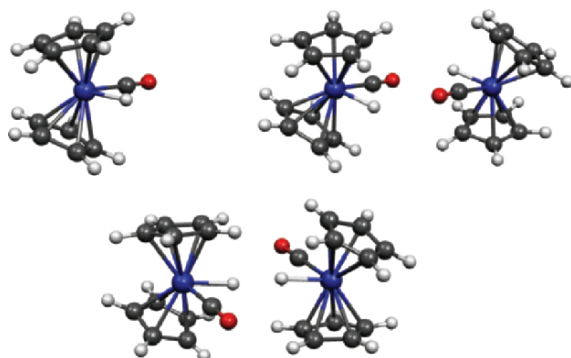
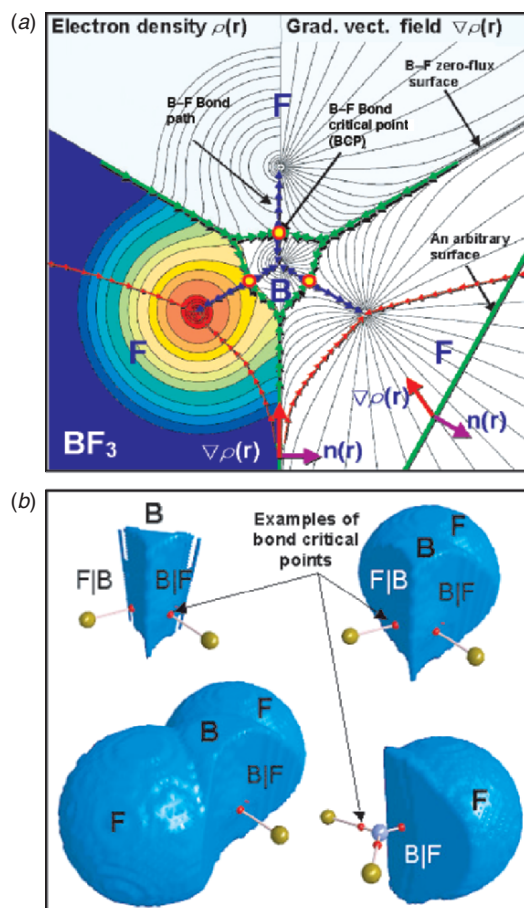


Figure 6-8. The x-ray structure of the monomer  $[(\eta^5\text{-C}_5\text{H}_5)_2\text{MoH}(\text{CO})]^+$  (top, left), the monoclinic form (top, right) and the triclinic form (bottom).



*Figure 9-1. (a) Plot of the electron density distribution (left) and of the associated gradient vector field of the electron density (right) in the molecular plane of  $\text{BF}_3$ . The lines connecting the nuclei (denoted by the blue arrows) are the lines of maximal density in space, the B-F bond paths, and the lines delimiting each atom (green arrows) are the intersection of the respective interatomic zero-flux surface with the plane of the drawing. The density contours on the left part of the figure increase from the outermost 0.001 au isodensity contour in steps of  $2 \times 10^n$ ,  $4 \times 10^n$ , and  $8 \times 10^n$  au with  $n$  starting at  $-3$  and increasing in steps of unity. The three bond critical points (BCPs) are denoted by the small red circles on the bond paths. One can see that an arbitrary surface does not satisfy the dot product in Eq. 1 since in this case the vectors are no longer orthogonal. (b) Three-dimensional renderings of the volume occupied by the electron density with atomic fragments in the  $\text{BF}_3$  molecule up to the outer 0.002 au isodensity surface. The interatomic zero-flux surfaces are denoted by the vertical bars between the atomic symbols, F|B. The large spheres represent the nuclei of the fluorine atoms (golden) and of the boron atom (blue-grey). The lines linking the nuclei of bonded atoms are the bond paths and the smaller red dots represent the BCPs.*

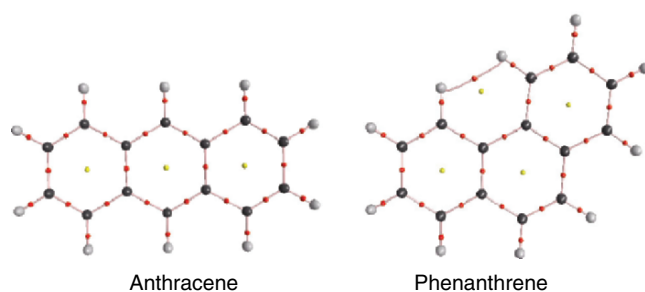


Figure 9-3. Molecular graphs of the two isomers anthracene and phenanthrene. The lines linking the nuclei are the bond paths, the red dots on the bond paths are the BCPs, and the yellow dots are the ring critical points (RCPs). The H–H bond path between H4 and H5 exists only in phenanthrene.

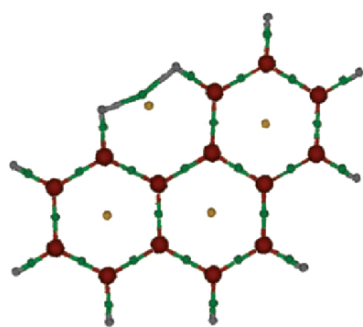


Figure 9-5. The virial graph of phenanthrene.

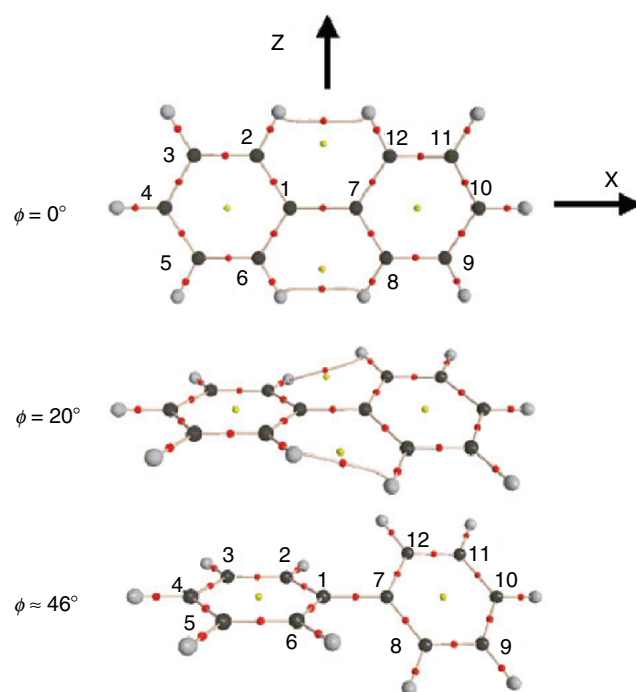


Figure 9-6. Molecular graphs of biphenyl as functions of the dihedral angle between the ring planes ( $\phi$ ). The coordinate system is indicated along with the atom numbering system. Hydrogen atoms take the same number as the carbon atoms to which they are bonded. At the critical value of  $\phi \approx 27^\circ$  there is a sudden “catastrophic” change in structure with the rupture of the two H–H bond paths (H2–H12 and H6–H8).

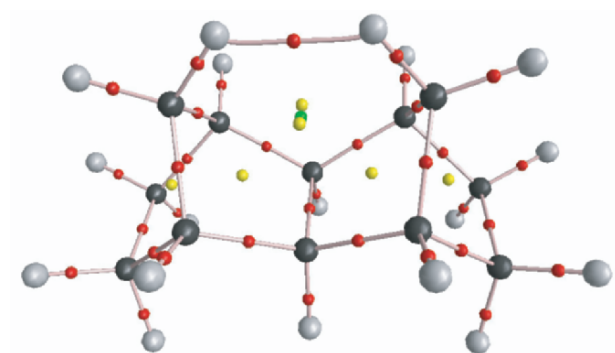


Figure 9-9. The calculated molecular graph of *exo, exo*-tetracyclo[6.2.1.1<sup>3,6</sup>.0<sup>2,7</sup>] dodecane which consists of two fused norbornanes rings. The H–H bond path links the nuclei of the two bridgehead hydrogen atoms. This results in the closure of two rings concomitant with the appearance of two ring critical points (yellow) and a cage critical point between them (green).

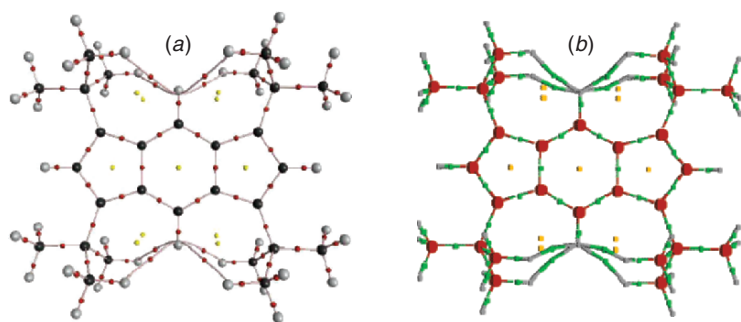


Figure 9-10. The calculated molecular graph (a) and its corresponding virial graph (b) of tetra-*tert*-butylindacene.

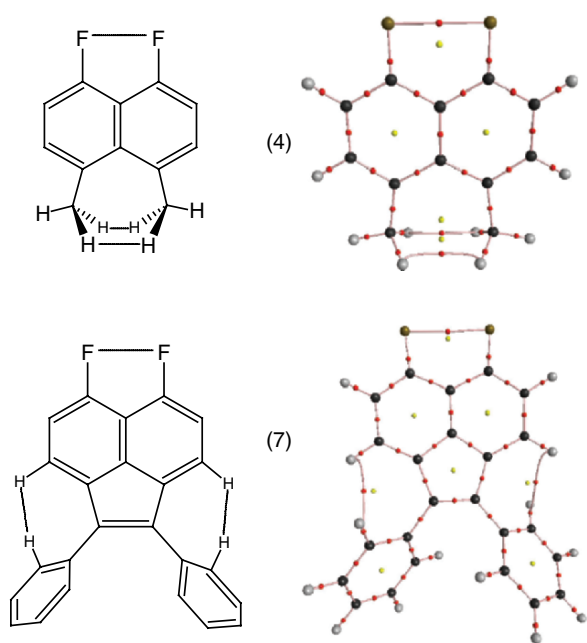
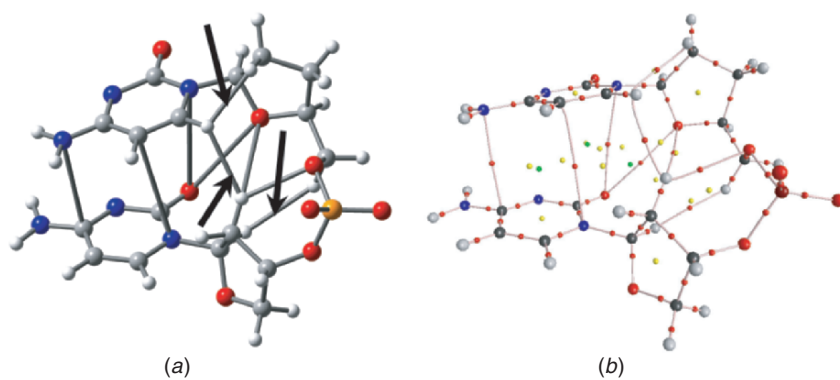
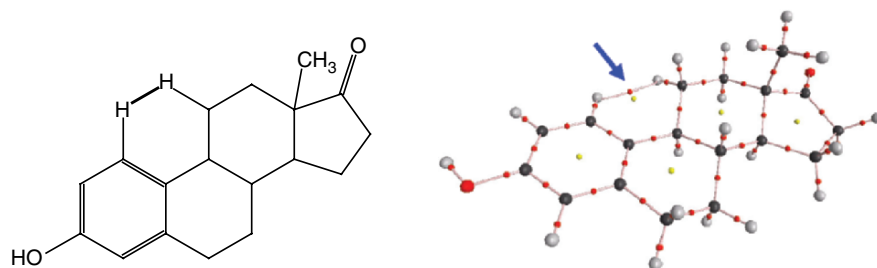


Figure 9-11. The chemical structure and the molecular graph of compounds (4) and (7) exhibiting  $C(sp^3)-H \cdots H-C(sp^3)$  and  $C(sp^2)-H \cdots H-C(sp^2)$  bond paths, respectively (adapted after Ref. [40]).



*Figure 9-12.* An idealised (a) and actual (b) molecular graph of a piece of DNA consisting of two consecutive cytosine bases attached to the phosphate-sugar backbone along a strand of DNA showing the several closed-shell interactions including three H–H bond paths (indicated by the arrows). (Adapted after Ref. [27].)



*Figure 9-13.* Example of a H–H bond path in biological molecules. The chemical structure and the molecular graph of the hormone estrone (the blue arrow indicates the H–H bond path) (adapted from Ref. [133]).



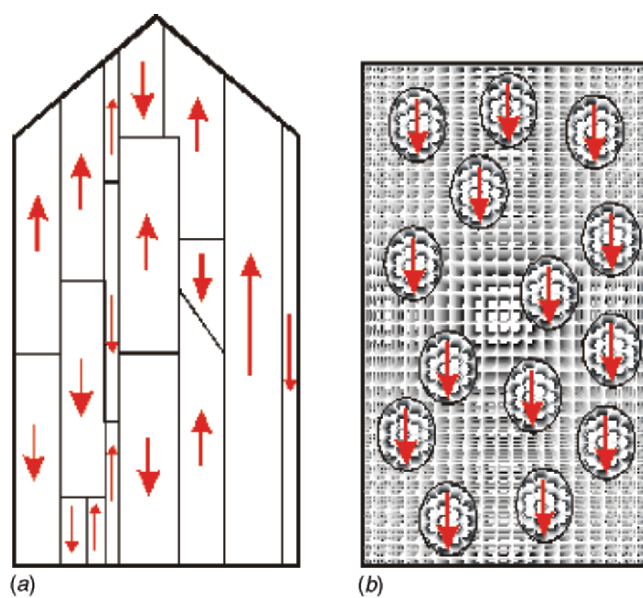


Figure 13-3. A schematic illustration of the domain structure in a ferroelectric crystal (a), and of a relaxor with the polarization of nanoregions pooled in one direction (b).

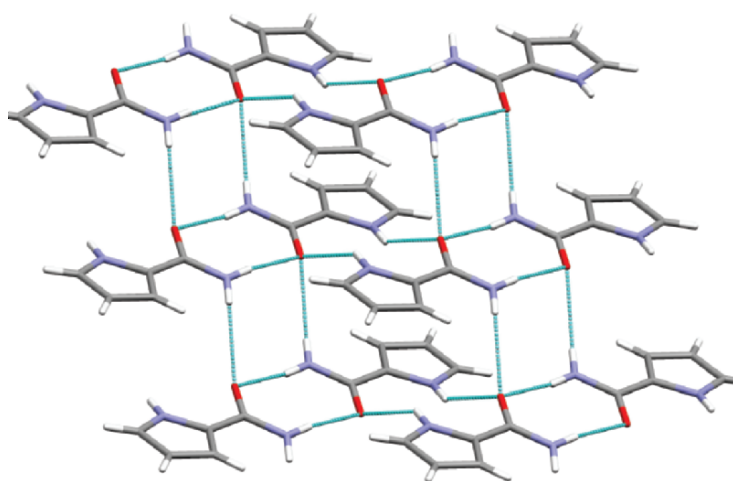


Figure 14-12. Pyrrole-2-Carboxamide—crystal structure motif containing centrosymmetric dimers with double N-H...O H-bonds.

# CONTENTS

Preface .....	v
1. Characterization of Hydrogen Bonding: From van der Waals Interactions to Covalency .....	1
<i>R. Parthasarathi and V. Subramanian</i>	
2. Intramolecular Hydrogen Bonds. Methodologies and Strategies for Their Strength Evaluation .....	51
<i>Giuseppe Buemi</i>	
3. Changes of Electron Properties in the Formation of Hydrogen Bonds .....	109
<i>Luis F. Pacios</i>	
4. Weak to Strong Hydrogen Bonds .....	149
<i>Han Myoung Lee, N. Jiten Singh, and Kwang S. Kim</i>	
5. The Nature of the C–H···X Intermolecular Interactions in Molecular Crystals. A Theoretical Perspective ....	193
<i>Juan J. Novoa, Fernando Mota, and Emiliana D'Oria</i>	
6. Weak Hydrogen Bonds Involving Transition Elements .....	245
<i>Maria José Calhorda</i>	
7. Contribution of CH···X Hydrogen Bonds to Biomolecular Structure .....	263
<i>Steve Scheiner</i>	
8. Neutral Blue-Shifting and Blue-Shifted Hydrogen Bonds .....	293
<i>Eugene S. Kryachko</i>	
9. Hydrogen–Hydrogen Bonding: The Non-Electrostatic Limit of Closed-Shell Interaction Between Two Hydrogen Atoms. A Critical Review .....	337
<i>Chérif F. Matta</i>	
10. Potential Energy Shape for the Proton Motion in Hydrogen Bonds Reflected in Infrared and NMR Spectra .....	377
<i>Gleb S. Denisov, Janez Mavri, and Lucjan Sobczyk</i>	
11. Molecular Geometry—Distant Consequences of H-Bonding .....	417
<i>Tadeusz M. Krygowski and Joanna E. Zachara</i>	

12.	Topology of X-Ray Charge Density of Hydrogen Bonds.....	441
	<i>Tibor S. Koritsanszky</i>	
13.	Structure–Property Relations for Hydrogen-Bonded Solids .....	471
	<i>A. Katrusiak</i>	
14.	Unrevealing the Nature of Hydrogen Bonds: $\pi$ -Electron Delocalization Shapes H-Bond Features. Intramolecular and Intermolecular Resonance-Assisted Hydrogen Bonds.....	487
	<i>Śławomir J. Grabowski and Jerzy Leszczynski</i>	
	Index .....	513

## CHAPTER 1

### CHARACTERIZATION OF HYDROGEN BONDING: FROM VAN DER WAALS INTERACTIONS TO COVALENCY

*Unified picture of hydrogen bonding based  
on electron density topography analysis*

R. PARTHASARATHI and V. SUBRAMANIAN

*Chemical Laboratory, Central Leather Research Institute, Adyar, Chennai 600 020, India*

**Abstract** This chapter reviews different aspects of hydrogen bonding (H-bonding) interaction in terms of its nature, occurrence, and other characteristic features. H-bonding is the most widely studied noncovalent interaction in chemical and biological systems. The state-of-art experimental and theoretical tools used to probe H-bonding interactions are highlighted in this review. The usefulness of electron density topography in eliciting the strength of the H-bonding interactions in a variety of molecular systems has been illustrated.

**Keywords:** Hydrogen bond; AIM; electron density; Laplacian of electron density; water; DNA; protein.

## 1 INTRODUCTION

Hydrogen bonding (H-bonding) is an intensively studied interaction in physics, chemistry and biology, and its significance is conspicuous in various real life examples [1]. Understanding of H-bonding interaction calls for inputs from various branches of science leading to a broad interdisciplinary research. Numerous articles, reviews, and books have appeared over 50 years on this subject. As a complete coverage of the voluminous information on this subject is an extremely difficult task, some recent findings are presented in this chapter.

The multifaceted nature of H-bonding interaction in various molecular systems has been vividly explained in the classical monographs on this interesting topic [2, 3]. Different quantum chemical approaches which predict the structure, energetics, spectra, and electronic properties of H-bonded complexes

were systematically presented in the monograph by Scheiner [4]. These monographs cover several important aspects of H-bonding, indicating the mammoth research activity in this field. It is clearly evident from the history of H-bonding that Pauling's book on *The Nature of the Chemical Bond* attracted the attention of the scientific community [5]. Currently, the term "Hydrogen Bonding" includes much of the broader spectrum of interactions found in gas, liquid, and solid states in addition to the conventional ones. In order to investigate this interaction, several experimental and theoretical methods have been used [1–4]. With the advances in experimental and computational techniques, it is now possible to investigate the nature of H-bonding interaction more meticulously. Bader's theory of atoms in molecules (AIM) [6] is one of the widely used theoretical tools to understand the H-bonding interaction. The present review is focused on applications of AIM theory and its usefulness in delineating different types of H-bonded interaction.

The outline of this chapter is as follows: The chapter begins with the classical definition of H-bonding. Its importance in molecular clusters, molecular solvation, and biomolecules are also presented in the first section. A brief overview of various experimental and theoretical methods used to characterize the H-bonding is presented in the second section with special emphasis on Bader's theory of AIM [6]. Since AIM theory has been explained in numerous reviews and also in other chapters of this volume, the necessary theoretical background to analyze H-bonding interactions is described here. In the last section, the salient results obtained from AIM calculations for a wide variety of molecular systems are provided. The power of AIM theory in explaining the unified picture of H-bonding interactions in various systems has been presented with examples from our recent work.

### 1.1 Classical Definition and Criteria of Hydrogen Bonding

H-bond is a noncovalent, attractive interaction between a proton donor X–H and a proton acceptor Y in the same or in a different molecule:



According to the conventional definition, H atom is bonded to electronegative atoms such as N, O, and F. Y is either an electronegative region or a region of electron excess [1–5, 7]. However, the experimental and theoretical results reveal that even C–H can be involved in H-bonds and  $\pi$  electrons can act as proton acceptors in the stabilization of weak H-bonding interaction in many chemical systems [3, 4]. In classical H-bonding, there is a shortening of X $\cdots$ Y distance, if X–H is H-bonded to Y. The distance between X $\cdots$ Y is less than the sum of the van der Waals radii of the two atoms X and Y. H-bonding interactions lead to increase in the X–H bond distance. As a consequence, a substantial red shift (of the order of 100 cm<sup>–1</sup>) is observed in the fundamental X–H stretching vibrational frequencies. Formation of the X–H $\cdots$ Y bond

decreases the mean magnetic shielding of proton involved in the H-bonding thus leading to low field shift [8, 9]. The low field shift in H-bonded complexes is about few parts per million and the anisotropy of the proton magnetic shielding can be increased by as much as 20 parts per million [10–12].

The strength of the strong H-bonding interactions ranges from 15.0 to 40 kcal/mol [1–4]. For the moderate (conventional) and weak H-bonds, the strengths vary from 4–15 to 1–4 kcal/mol, respectively. The strength of H-bonded interactions in diverse molecular systems has been classified [2, 13, 14]. Desiraju has proposed a unified picture of the H-bonding interactions in various systems and the concept of “hydrogen bridge” [14]. The three types of H-bonding interactions which are most often discussed in the literature are weak, moderate, and strong. The properties of these three types are listed in Table 1.

The H-bond strength depends on its length and angle and hence, it has directionality. Nevertheless, small deviations from linearity in the bond angle (up to 20°) have marginal effect on H-bond strength. The dependency of the same on H-bond length is very important and has been shown to decay exponentially with distance. The question on “what is the fundamental nature of hydrogen bond?” has been the subject of numerous investigations in the literature [1–4]. In a classical sense, H-bonding is highly electrostatic and partly covalent. From a rigorous theoretical perspective, H-bonding is not a simple interaction. It has contributions from electrostatic interactions (acid/base), polarization (hard/soft) effects, van der Waals (dispersion/repulsion: intermolecular electron correlation) interactions and covalency (charge transfer)[14].

## 1.2 Nature of Conventional and Improper or Blue Shifting Hydrogen Bonding

It is evident from the conventional definition of H-bonding that formation of  $X-H \cdots Y$  bond is accompanied by a weakening of the covalent  $X-H$  bond with concomitant decrease of  $X-H$  stretching frequency [1–4, 13, 14]. This red shift

Table 1. General characteristics of the three major types of H-bonds. The numerical information shows the comparative trends only [13]

H-bond parameters	Strong	Moderate	Weak
Interaction type	Strongly covalent	Mostly electrostatic	Electrostatic/dispersed
Bond lengths ( $H \cdots Y$ [Å])	1.2–1.5	1.5–2.2	>2.2
Lengthening of $X-H$ (Å)	0.08–0.25	0.02–0.08	<0.02
$X-H$ Vs. $H \cdots Y$	$X-H \approx H \cdots Y$	$X-H < H \cdots Y$	$X-H \ll H \cdots Y$
H-bond length ( $X \cdots Y$ [Å])	2.2–2.5	2.5–3.2	>3.2
Directionality	Strong	Moderate	Weak
H-bond angles (°)	170–180	>130	>90
H-bond strength (kcal/mol)	15–40	4–15	<4
Relative Infrared shift ( $cm^{-1}$ )	25%	10–25%	<10%

belongs to one of the most important characteristics of the H-bonding interaction. Its other signature is the considerable increase in the intensity of the spectral band connected with X–H stretching frequency. In addition, there is a nonnegligible electron density transfer from a proton acceptor to a donor [15]. Electron density is transferred from the proton acceptor (lone pair) to the  $\sigma^*$ -antibonding orbital of X–H bond, which causes a weakening and elongation of this bond and a decrease in the X–H stretch frequency.

On the contrary, there are some typical situations, wherein the X–H bond gets compressed and the corresponding X–H stretching vibration is shifted to a higher frequency. This type is called as blue shifting or improper or anti-H-bonding. A review on this appeared recently [16]. One of the first experimental evidences of blue shift in X–H stretching frequency upon formation of a complex was observed by Sandorfy and coworkers [17]. The other experimental evidence for blue shift was noted by Arnold and coworkers who measured the blue shift of C–H stretch of chloroform–triformylmethane complexation [18]. In 1997, Boldeshul et al. have reported the blue shift in the H-bonded complexes of haloforms with various proton acceptors [19]. The first theoretical study on blue shifted H-bonded systems has been performed by Hobza et al. [20]. Subsequently numerous theoretical studies have been carried out to understand the blue shifted H-bonding interaction [21–45]. The electronic basis for improper H-bonding has been analyzed by Alabugin et al. [46]. The observed structural reorganization of X–H bond in both proper and improper H-bonding arises from a balance of hyperconjugative bond weakening and rehybridization bond strengthening. Improper H-bonding is likely to be seen only when the X–H bond elongating hyperconjugative  $n(Y) \rightarrow \sigma^*(X-H)$  interaction is relatively weak. When the hyperconjugative interaction is weak and the X-hybrid orbital in X–H bond is able to undergo a sufficient change in hybridization and polarization, rehybridization dominates leading to a shortening of the X–H bond and a blue shift in the X–H stretching frequency. It has been shown that improper H-bonding is not an unexpected aberration but rather a logical consequence of Bent's rule in structural organic chemistry, which predicts an increase in s-character in X–H bonds upon H-bond formation, because H becomes more electropositive during this process [46].

### 1.3 Hydrogen Bonding in Molecular Dimers

Numerous H-bonded homodimers and heterodimers have been investigated using ab initio electronic structure calculations and density functional theory (DFT)-based methods [1–4]. Various aspects of H-bonding starting from classical definition to H-bonded dimers have been discussed in one of the earlier reviews by Kollman and Allen [47]. Water dimer is a typical example used to explain the H-bonding interaction. The structure of the water dimer was analyzed by a molecular beam electric resonance experiment [48, 49]. Almost all theoretical methods developed so far have been employed to predict the

structure and energetics of H-bonding interaction in water [1–4, 50–63]. All types of basis sets including Pople’s and Dunning’s correlation consistent basis sets have been used to calculate the structure and energetics of the water dimer [64]. The predictive power of the DFT-based methods have also been systematically analyzed by taking the water dimer as an example. The calculated H-bond strength in the water dimer obtained from various levels of calculations is represented in Table 2.

It is evident from the large scale ab initio molecular orbital calculations that the best estimate of strength of H-bond energy of water dimer is  $5.0 \pm 0.1$  kcal/mol [58]. Correcting this value for zero-point and temperature effects yields the value around  $\Delta H(375) = -3.2 \pm 0.1$  kcal/mol. This value is within the error limits of the best experimental estimate of  $-3.6 \pm 0.5$  kcal/mol. From the analysis of DFT results, it is found that the hybrid methods provide overall description of properties of the H-bonded water dimer [64].

Extensive work on the H-bonding in dimers is presented in previous original articles and reviews [1–4, 7, 13, 65–74]. Dimers of methanol, formaldehyde, formamide, formic acid, acetic acid, *N*-methylacetamide, phenol, etc., have been studied using a variety of quantum chemical methods. Some of these dimers have been chosen as model systems to understand the H-bonding interactions in biomolecules. Geometries, energetics, vibrational frequencies, and electronic properties of H-bonded dimers were investigated [4]. The strengths of O–H...O–H, O–H...N–H, N–H...O–C, C–H...O–C,  $\pi$ ...O–H,  $\pi$ ...H–N,  $\pi$ ...H–C, and  $\pi$ – $\pi$  interactions have been predicted from these calculations. The analysis clearly depicts the presence of different kind of interactions found in the various homodimer and heterodimer models. From these studies, it is possible to understand the multifarious interactions in stabilization and structure of biomolecules.

Table 2. Counterpoise corrected stabilization energy (kcal/mol) of the water dimer calculated at different levels of theory

Basis set	Methods			
	HF	MP2	CCSD(T)	DFT(B3LYP)
6-31G*	4.75	5.12	–	4.75
6-31G**	4.56	4.69	–	5.1
6-31 + G**	4.44	4.81	–	5.24
6-31 + +G**	4.42	4.79	–	5.22
6-311 + +G**	4.27	4.48	–	5.07
cc-pVDZ	3.6	3.9	3.7	–
cc-pVTZ	3.5	4.4	4.3	4.5
cc-pVQZ	3.5	4.7	4.7	4.6
aug-cc-pVDZ	3.5	4.3	4.3	4.5
aug-cc-pVTZ	3.5	4.6	4.7	4.6
aug-cc-pVQZ	3.5	4.8	4.9	4.6



#### 1.4 Hydrogen Bonding in Molecular Hydration and Microsolvation

Solvation of neutral and charged molecules is a process which is of fundamental importance to many phenomena in chemistry and biology [75]. In the literature, molecular hydration, molecular solvation, and microsolvation are the frequently used terms to describe the interaction of solvent molecules with solute. In order to study the solvation process, isolated size-selected clusters of the type  $M-S_n$  have been frequently used as models to characterize the stepwise molecular hydration of molecule (M) by solvent (S). The fruitful combination of mass spectrometric and other spectroscopy techniques on the experimental side, and electronic structure calculations on the other side has been shown to be a powerful strategy [76]. Several investigations describing the solvation of molecules using different quantum chemical calculations and classical approaches have been reported [77–80]. In the prediction of effect of solvation, two approaches viz continuum solvation model (implicit solvation) and direct interaction of solvent molecules with solute (discrete model) have been used [80, 81]. The continuum solvation model treats the solvent as a continuous dielectric medium that reacts with solute charge distribution. Self-consistent reaction field (SCRF) model developed from the original works of Born–Onsager and Kirkwood is now used for modeling the bulk effect of solvation [82–86]. Various implicit models employed to treat molecular solvation or hydration have been reviewed in detail [77–80]. However, continuum models do not take into account of the specific H-bonding interactions of solvent molecules with solutes. In order to elicit the molecular hydration process, explicit interaction of solvent molecules with the solute has been considered. To probe these interactions, a variety of models have been proposed. Buckingham–Fowler model [87], Molecular Mechanics for Clusters (MMC) and Dykstra [88], Alhambra, Luque and Orozco model [89], Polarizable Atomic Multipole Model [90], and Electrostatic Potential for Intermolecular Complexation (EPIC) [91, 92] are some of the popular strategies used to study these weak interactions in solute–solvent.

EPIC model originated from the pioneering work of Gadre and his group and it exploits rich topographical features of molecular electrostatic potential (MESP) [91–98]. Several theoretical methodologies combined with MESP topography have been used to investigate molecular hydration processes [97–104]. Recently, the success of the EPIC model along with other quantum chemical investigations on explicit molecular hydration processes has been reviewed by Gadre et al. [98]. MESP topography of molecules has been found to give information on the probable sites of water molecule interaction in the both polar and nonpolar molecules. Different classes of examples starting from small molecules to large clusters have been investigated in detail using EPIC and quantum chemistry tools. In the microsolvation of nonpolar molecules, benzene was used as a prototype molecule. Numerous experimental and theoretical methods have been employed to understand the hydration process in benzene.

Experimental and theoretical results on microsolvation of benzene were summarized by Brutschy [105]. Infrared (IR) spectral investigations of benzene–(H<sub>2</sub>O)<sub>8</sub> have clearly revealed the changes in the structural features of water clusters in the presence of benzene. Zwier has reported the detailed analysis on the IR spectra of large size solvated clusters [106].

The structures and properties of isolated, solvated, and complexed nucleic acid bases have been reviewed by Leszczynski [107]. Interaction of water molecules with various DNA bases, base pairs, and DNA stacks has also been studied to understand structure, nonplanarity bases, tautomerism, and stability. Gadre et al. have also studied the solvation of biomolecules using the EPIC-based docking followed by *ab initio* and DFT methods [98]. The gas phase hydration of cytosine base, cytosine–cytosine H-bonded base pairs (CC), and cytosine–cytosine stacked dimer (C/C) using *ab initio* calculations have been reported by our group [108, 109]. Using the topological features of MESP, starting geometries for *ab initio* calculations have been generated using the EPIC model for interaction of water molecules with cytosine (C), cytosine–cytosine H-bonded pair (CC), and stacked dimer (C/C). The calculated interaction energies of hydrated stacked C/C dimer are numerically higher than that predicted for hydrated CC pair and the difference in the energy ranges from 1 to 2.5 kcal/mol at all levels of calculations explored [109]. Hence, it has been concluded that the stacked C/C dimer hydrates better than the H-bonded base pair, which is in agreement with the experimental evidence [110].

In addition to the microsolvation, the effect of solvation on the reaction has also been modeled by Re and Morokuma [111]. They demonstrated the significance of molecular solvation using the two-layered ONIOM method. The S<sub>N</sub>2 pathway between CH<sub>3</sub>Cl and OH<sup>−</sup> ion in microsolvated clusters with one or two water molecules has been studied. This work highlighted the role of solvent in the chemical reaction and also the power of ONIOM model to predict complex systems. All these studies have undoubtedly brought out the significance of H-bonding in solute–solvent interaction, chemical reactivity, and molecular solvation phenomenon.

## 1.5 Hydrogen Bonding in Biological Systems

### 1.5.1 In DNA and RNA base pairing

It is well documented that the H-bonding interaction is important for the structure and function of biomolecules [112, 113]. H-bonding in  $\alpha$ -helical and  $\beta$ -sheet structures in proteins by Pauling et al. [114], DNA base pairs by Watson and Crick [115], and triple helix of collagen by Ramachandran and Kartha [116], and simultaneously by Rich and Crick [117] have opened a new branch of science known as “structural biology.” The H-bonding interactions in nucleic acids play a crucial role in the double helical structure of DNA and RNA along with stacking interactions facilitating molecular recognition via

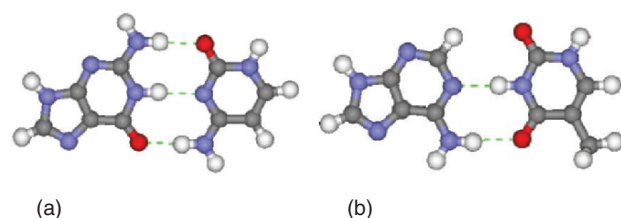


Figure 1. Hydrogen-bonded (a) G...C and (b) A...T DNA base pairs.

replication processes and protein synthesis [113]. Extensive theoretical methodologies have been used to derive information about the H-bonding in DNA base pairing and base stacking [118–134]. The representative H-bonded G...C and A...T DNA base pairs are shown in Fig. 1. The *ab initio* calculation on the G...C and A...T pairs provides the required information about the strength of H-bonding in these systems and the respective binding energies are 20.0 and 17.0 kcal/mol [118]. H-bonding is mainly accountable for the DNA–ligand recognition phenomenon and the studies on molecular recognition help to design new drug molecules [135].

Water is an essential part in the biomacromolecular system, which is mainly responsible for the structure and functions of nucleic acids, proteins, and other constituents of cell [136–138]. Both proteins and DNA are generally hydrated. It is well known that the conformation of DNA is sensitive to hydration, and presence of salts and ligand molecules [112, 138]. The nucleic acids have three levels of water structure. About 12 water molecules per nucleotide are involved in the primary hydration shell [107, 112, 137, 138]. The water molecules present in the primary shell are impermeable to cations and do not form ice on freezing. The secondary level is permeable to cations and forms ice on freezing and third level is the completely disordered, so-called bulk water. Several theoretical studies have been carried out on the level of hydration on DNA bases, base pairs, base stacks, and double helical DNA [107, 121, 131, 139]. Both the experimental and molecular simulation studies have clearly brought out the importance of hydration in DNA and RNA structures [140–147].

### 1.5.2 Hydrogen bonding in protein secondary structure

H-bonding is the most important interaction governing protein structure, folding, binding, enzyme catalysis, and other properties. The basic secondary structural elements in protein structure are  $\alpha$ -helix,  $\beta$ -sheet,  $\gamma$ -turn,  $\pi$ -helix, etc., which are stabilized by H-bonding interactions [1–3, 113, 136]. H-bonding in  $\alpha$ -helix and  $\beta$ -sheet is presented in Fig. 2.  $\alpha$ -Helix is a result of intramolecular H-bonded interaction between C = O group of the  $i$ th peptide residue with N–H group of the  $i + 4$ th residue in the peptide or protein sequence. In both the parallel and antiparallel  $\beta$ -sheets, the C = O of one peptide chain H-bonds with

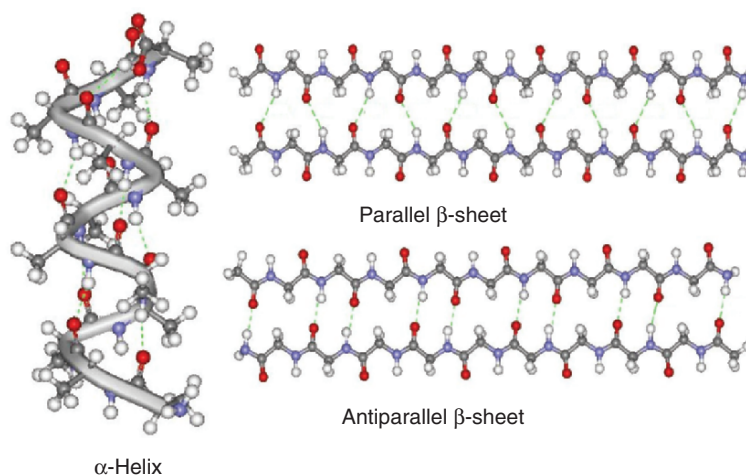


Figure 2 (see color section). Hydrogen bonding in various protein secondary structures.

N–H of the other chain in a unique fashion. H-bonding interaction along with other noncovalent interactions is mainly accountable for the interaction of DNA and protein with other molecules.

Making and breaking of H-bonding in a dynamics situation profoundly influence the rates of dynamics equilibria, which are of paramount importance for the biological activity of proteins [148]. The solvation dynamics of water structure around the protein have been studied in great detail with a view to gain insight into protein folding and enzyme action [84]. It was observed from the atomistic simulation on the explicitly solvated protein that the structural relaxation of protein–water H-bonds is much slower than that of the water–water H-bonds [149].

### 1.6 Hydrogen Bonding in Crystal Engineering

Crystal structure arises as a result of intermolecular interactions and packing. The packing interaction is a convolution of a large number of strong and weak interactions, each of which influences the other closely [3]. Small changes in the molecular structure lead to observable changes in the crystal structure. Generally, there is no obvious relationship between molecular structure and crystal structure. In crystal engineering, attempts have been made to design molecular systems which could throw light on how molecular structure is related to crystal structure. Both the strong and weak H-bonded interactions play a dominant role in engineering of crystals. The role of weak H-bonded interactions in various molecules and crystals has been dealt with in a recent monograph [3].

## 2 EXPERIMENTAL AND THEORETICAL METHODS IN UNRAVELING H-BONDED COMPLEXES

### 2.1 Experimental Methods

The descriptions of the structure, energy, and dynamics of H-bonds continue to be a formidable task for both experimental and theoretical investigations. IR and nuclear magnetic resonance (NMR) techniques have become routine tools to analyze H-bonding interactions in various systems [1–4, 150]. The vibrational modes of molecules in the H-bonded state are affected in several ways. The proton involved in H-bonding interaction exhibits down field shift. Spectroscopic information obtained from these techniques has been used to probe H-bonding interactions.

Various experimental methods used to investigate the H-bonded clusters in gas phase are described in the earlier reviews [150–152]. Since molecular clusters are produced in supersonic beams in the gas phase under collision free conditions, they are free from perturbation of many-body interactions. The spectroscopic characterization of these clusters has less complexity. Hence, high level quantum chemical calculations on these clusters can be directly compared with the experimental values. Due to advent of laser-based techniques, it is currently possible to study the size and mass selective molecular clusters produced in supersonic beam. The combination of high resolution spectroscopy along with the mass and size selective strategies has enabled the scientific community to look at the intrinsic features of H-bonding. Principles behind the method of size selection, beam spectroscopy, and experimental setup have also been thoroughly described in an earlier thematic issue in “chemical review” [105, 150–152].

Challenges in experiments and theory to probe the noncovalent interactions in the weakly bonded clusters have been critically reviewed by Muller-Dethlefs and Hobza [150]. They highlighted the importance of microwave, vibrational rotation tunneling (VRT), REMPI and hole burning, and zero kinetic energy (ZEKE) spectroscopies in probing the noncovalent interactions in molecular clusters in gas phase [150]. IR spectroscopy of size-selected water and methanol clusters was discussed by Buck and Huisken [151]. Brutschy [105] has provided an account on the structural aspects of aromatic molecules surrounded by several polar molecules using IR double resonance laser spectroscopy (IR/R2PI ion depletion spectroscopy) along with the important computational results [105]. Neusser and Siglow have discussed the applications of high resolution ultraviolet (UV) spectroscopy to study the neutral and ionic H-bonded clusters [152]. Mikami have brilliantly exploited the beam spectroscopy to study the H-bonded clusters in the gas phase [153–163]. From their studies, it is possible to gain new insight into the structure and dynamics of H-bonded phenol and protonated water clusters. IR spectroscopy study on  $\text{H}_3\text{O}^+(\text{H}_2\text{O})_n$  by them clearly elucidated that the small-sized clusters develop into a two-

dimensional network whereas large clusters with  $n \geq 21$  form nanometer-scaled cages [163].

Recently, large  $(\text{H}_2\text{O})_n$  clusters with ranges  $n$  from 20 to 1960 have been investigated by Steinbach et al. using photofragment spectroscopy [164, 165]. They measured the vibrational spectra of the size-selected water hexamer and identified the H-bonded open book arrangement in the cluster with temperature range from 40 to 60 K [165]. Jordan, Zwier and their collaborators have made several noteworthy contributions to this contemporary area by successful combination of sophisticated experimental and theoretical methods to a large number of H-bonded clusters [106, 166–177]. Their studies include neutral and charged water clusters in various structural environments. The IR spectra have been used to probe the issues related to solvation of Eigen vs. Zundel cation [173]. Headrick et al. have reported how the vibrational spectrum of protonated water clusters evolves in size ranging from 2 to 11 water molecules [177]. IR signature bands indicated the limiting forms of embedded Eigen or Zundel forms in the respective spectra.

## 2.2 Theoretical Methods

A variety of theoretical methodologies are available at different theoretical levels and accuracy. Different quantum chemical methods used to analyze H-bonding interactions have been systematically discussed by Scheiner in his monograph [4]. Starting from semi-empirical molecular orbital methods, Hartree–Fock (HF), and post-HF methodologies have been employed to study H-bonding. HF method treats the exchange term appropriately and thus it predicts reasonably the electrostatic contribution to the strength of H-bonding. The need for treatment of post-HF techniques for H-bonded systems has been observed as discussed in recent monographs [1–4]. The inclusion of electron correlation and hence intermolecular dispersion energy becomes considerably important for the prediction of strength of the H-bonding. Møller–Plesset (MP2), coupled-cluster singles doubles (CCSD), and CCSD with noniterative triples correction (CCSD (T)) methods are widely used methodologies to investigate H-bonding interactions. The implementation of DFT formalism in the Gaussian package has made it possible to investigate the utility of several exchange and correlational functionals in the prediction of H-bonding [178, 179]. Recently, Zhao and Truhlar have investigated the usefulness of DFT functionals in the prediction of H-bonding [180]. It is a well-known fact that the basis set used in the calculation significantly influences the calculated bond length, bond angle, electronic properties, interaction energy, and vibrational spectra [180]. Hence, theoretically, different combinations of methodologies and basis sets have been applied to obtain reliable estimates of geometrical parameters and energetics of H-bonded systems. In addition, the interaction energy obtained from these calculations needs to be corrected for basis set superposition error (BSSE) as suggested by Boys and Bernardi [181].